

POSSIBLE EFFECTS OF TEXTURE AND TEXTURE GRADIENTS ON ALUMINUM
REFERENCE STANDARDS

R.B. Mignogna

Mechanics of Materials Branch
Naval Research Laboratory
Washington, DC 20375-5000

K.R. Bernetich

Naval Sea Systems Command
Washington, DC 20362-5101

S.D. Hart

Ultrasonics Consultancy
4513 Apple Tree Dr.
Alexandria, VA 22310

INTRODUCTION

The ultrasonic NDT community has been aware for several years that a different Index Point is found for angle beam search units when comparing aluminum IIW type calibration blocks with steel blocks of identical design. Brissaud and Kleiman [1,2] and Watson [3] have discussed anisotropy texture as a possible cause of the difference.

Figure 1 shows the basic design of the IIW block. The principal application of the IIW block is the determination of the Beam Exit Point (BEP) on the shoe of an angle beam wedge. The IIW block is also used for the determination (or verification) of the angle of refraction of the ultrasonic beam in the block material. To find the BEP, the probe is placed in the vicinity of point A (Fig. 1) with the beam directed toward the quadrant at the right end of the block. Point O is the center of curvature of the quadrant. At point O, if the IIW block is isotropic, the ultrasonic beam should be along a radius of the quadrant. The probe, used in a pulse echo mode, is moved back and forth to obtain the maximum reflection from the quadrant surface. At this point, the BEP is said to lie opposite point O. An index mark is made on side of the probe opposite point O. This defines the Beam Index for the transducer.

One consequence of anisotropy is that the group velocity (energy) vector deviates from the phase vector when the latter does not coincide with a symmetry direction. The probe must be adjusted for maximum reflection of the energy vector, for it carries the information. To accomplish this the probe must be displaced some distance from point O. The amount that the BEP is displaced from point O is called the 'index shift'.

The index shift demonstrates the importance of isotropy in calibration blocks. Conversely, it is also important to know the state of anisotropy in any material to be examined. Although hot rolled steel can

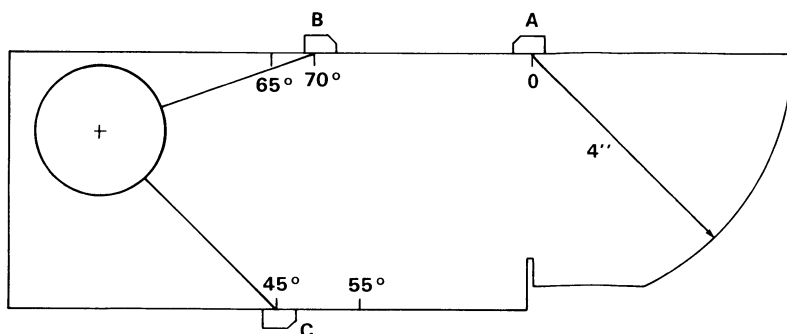


Fig. 1. Schematic diagram of the IIW type calibration block.

be made nearly isotropic, cold rolled steel plate shows considerable anisotropy. The beam angles in the cold rolled steel plate may differ noticeably from the angle determined from a steel calibration block.

To analytically demonstrate the index shift due to anisotropy or texture, ultrasonically measured orientation distribution function coefficients are used in the forward calculations of both the phase and energy vectors. These results are applied to the BEP calibration procedure. Measurements made at several depths in a 51 mm thick rolled aluminum plate show texture variation through the thickness. The possible influences of these variations are discussed.

QUANTITATIVE ASSESSMENT OF TEXTURE (THEORY)

To determine and understand the effects texture has on ultrasonic calibration blocks or reference standards it is necessary to have a means of quantitatively assessing the texture. For ultrasonic measurements of rolled plates of materials having a cubic single crystal structure, Sayers has shown that texture can be described (approximated) as an orthotropic distribution of cubic crystallites.[4] These materials include but are not limited to most commercial polycrystalline aggregates of aluminum, aluminum alloys, iron and steels. The reader is directed to the work of Sayers for both the theory and further references. Only the results pertinent to this paper will be described here.

The use of Orientation Distribution Functions (ODF) permits the texture to be quantitatively described in terms of the coefficients of the ODF. The ODF, as the name implies, is a mathematical representation of the distribution of the orientation of the grains (polycrystals) referenced to the rolling and transverse direction of the rolled plate. Ultrasonic texture measurements require only three of these coefficients, W_{400} , W_{420} and W_{440} .

The material used in this study was a 51 mm thick rolled plate of 2024-T4 aluminum. The orthotropic symmetry directions are shown in Fig. 2 with respect to the rolling direction. The elastic constants of the rolled material (orthotropic), C'_{ij} can be written in terms of the cubic elastic constants (C_{11} , C_{12} and C_{44}) and the texture coefficients (W_{400} , W_{420} and W_{440}) as shown in Eqs. 4 and 10 of Ref. 4.

Using Eqs. 4 and 10, of Ref. 4, the three phase velocities, v_{ij} , along each of the x_3 , x_1 and x_2 directions can be written in terms of the cubic elastic constants, density ρ and the texture coefficients as:

$$v_{33}^2 = \{C_{11} - 2(C_{11} - C_{12} - 2C_{44})[B_1 - 8B_2W_{400}]\} / \rho \quad (1)$$

$$v_{31}^2 = \{C_{44} + (C_{11} - C_{12} - 2 C_{44}) [B_1 - 8 B_2 (W_{400}/\rho)\} \quad (2)$$

$$v_{32}^2 = \{C_{44} + (C_{11} - C_{12} - 2 C_{44}) [B_1 - 8 B_2 (W_{400} + B_3 W_{420})]\}/\rho \quad (3)$$

$$v_{11}^2 = \{C_{11} - 2 (C_{11} - C_{12} - 2 C_{44}) [B_1 - 3 B_2 (W_{400} - B_4 W_{420} + B_5 W_{440})]\}/\rho \quad (4)$$

$$v_{13}^2 = v_{31}^2 \quad (5)$$

$$v_{12}^2 = \{C_{44} + (C_{11} - C_{12} - 2 C_{44}) [B_1 - 2 B_2 (W_{400} - 3 B_5 W_{440})]\}/\rho \quad (6)$$

$$v_{22}^2 = \{C_{11} - 2 (C_{11} - C_{12} - 2 C_{44}) [B_1 - 3 B_2 (W_{400} + B_4 W_{420} + B_5 W_{440})]\}/\rho \quad (7)$$

$$v_{23}^2 = v_{32}^2 \quad (8)$$

$$v_{21}^2 = v_{12}^2 \quad (9)$$

where $c = C_{11} - C_{12} - 2 C_{44}$ and $B_1 = 1/5$, $B_2 = 2/35 \sqrt{2} \pi^2$, $B_3 = 2/3 \sqrt{10}$, $B_4 = 1/3 \sqrt{70}$ and $B_5 = \sqrt{5}/\sqrt{2}$.

The first subscript of the velocity indicates the propagation direction and the second denotes the polarization direction. If the elastic constants C_{11} , C_{12} and C_{44} and the density are known and the velocities experimentally determined, it should be possible to determine the three texture coefficients from three independent relations of Eqs. 1-9 for a homogeneous textured material.

QUANTITATIVE ASSESSMENT OF TEXTURE (EXPERIMENT)

Previous results have indicated that texture in rolled aluminum plate is 'reasonably' homogeneous in the plane of the plate but not, in general, homogeneous through the thickness of the plate. The variation through the thickness has been found to be symmetric about the center plane of the plate. This was assumed to be the case for the material used in this study. The plate was arbitrarily divided into four equal thicknesses on one side of the center plane. A total of six specimens were cut from the 51 mm thick plate of 2024-T4 aluminum as shown in Fig. 2. Four of the specimens were 'plate-like', having dimensions 51 x 51 x 6.3 mm, and cut at 6.3 mm intervals through the thickness of the plate from one side of the symmetry plane. The specimens are labelled A, B, C and D in Fig. 2 and called 'type 3' to correspond to the wave propagation direction. These specimens permitted measurement of three wave speeds in the x_3 direction for each of the four layers. Two other specimens were cut in such a manner that the six additional wave speeds, three in the x_1 (type 1) and three in the x_2 (type 2) direction, could also be measured in each layer. The specimens, along with the propagation and polarization directions of the measurable wave speeds, are shown in the lower right hand corner of Fig. 2. The 'layers' corresponding to the 'plate-like' specimens A through D are also shown and labeled on specimen type 1 and type 2 in the figure. The transducer was placed at the '*' for each layer. Standard machining practices were employed with no special precautions to ensure parallel surfaces or finish employed.

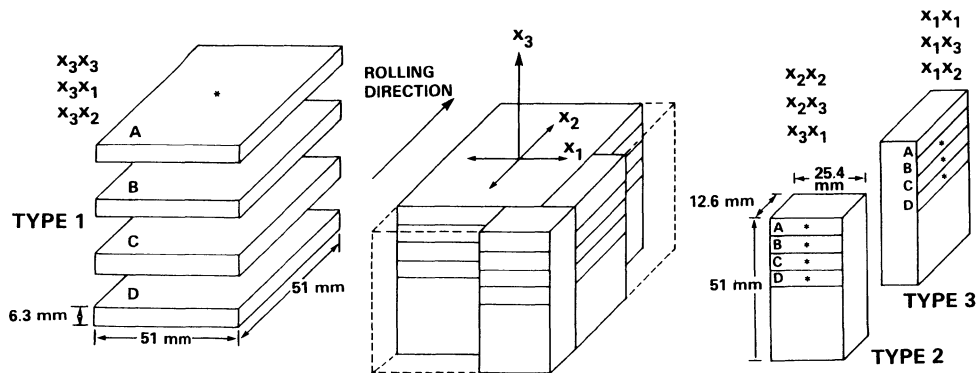


Fig. 2. Schematic diagram showing the orientation and dimensions of the specimens relative to the rolled 2024-T4 51 mm aluminum plate.

All nine velocities were determined for each layer. A minimum of five measurements were made and then averaged for each velocity. Absolute velocity measurements were made and the standard deviation of the measured velocities was approximately 0.1% for all four layers.

Data Analysis

In order to calculate the texture coefficients, ρ , C_{11} , C_{12} and C_{44} were assumed to be the single crystal values for pure aluminum. These values were obtained from the literature[5]. Using the experimentally determined velocities and the assumed values for the elastic constants and density, a number of sets of arbitrary combinations of three independent equations from Eqs. 1-9 were solved in order to obtain W_{400} , W_{420} and W_{440} . The values obtained from the various combinations of equations differed substantially from one another. These values were substituted back into Eqs. 1-9 and predicted velocities were calculated. The differences between the calculated and measured velocities were outside of the experimental error, all high or all low depending upon which calculated set of texture coefficients were used. It was determined that there are 51 combinations of three independent relations in Eqs. 1-9. In an attempt to use all the experimental data and average the texture coefficients, all 51 combinations of relations were solved and the values averaged. The averaged texture coefficients were then used to calculate velocity values. The calculated values were still outside of the experimental errors and felt to be unacceptable.

In this analysis two assumptions have been made that may introduce errors. The first assumption is that the plate has a single texture. The second is that the elastic constants have values of pure aluminum single crystal. The first assumption is more fundamental to the theory and more difficult to modify. The second, however, was an easier task to modify and seemed to be a likely candidate since 2024 is an aluminum alloy and not pure aluminum. An additional relation that can be used to reduce the number of elastic constants to two is shown in Eq. 22 of Ref. 4 and can be rewritten as:

$$C_{11} = \left[\sum_{i=1}^3 \left(\sum_{j=1}^3 v^2_{ij} - 2 C_{44} \right) \right] / 3 \quad (10)$$

in order to take advantage of all of the velocity data. This reduces the number of unknowns to five. However, there are not five independent relations in Eqs. 1-9.

A nonlinear least-squares method was used to determine both the elastic constants and texture coefficients. The method used may not be favorably looked upon by a mathematician, but did allow us to take advantage of the small amount of information available. The method entailed alternatively computing the error due to incorrect elastic constants and texture coefficients. The difference between the predicted velocities and the experimental velocities was calculated, first due to incorrect texture coefficients. A fraction of the correction term was added back in to the initial guess and then the same procedure was carried out for the elastic constants. This calculation sequence was repeated until both the texture coefficients and elastic constants converged. The elastic constants for pure aluminum and the average texture coefficients (described earlier) were used as a first guess for the least-squares program. The texture coefficients and elastic constants obtained in this manner are presented in Table I for all four layers. The single crystal values for pure aluminum used as the initial guess were $C_{11}=10.82$, $C_{12}=6.13$ and $C_{44}=2.85$ ($\times 10^{11}$ dyne/cm²). The values calculated for the elastic constants at the various layers differ by less than one percent of the initial guess. However, this caused as much as a 20% change in the texture coefficients. All of the velocities calculated from the values shown in Table I were within $\pm 2 \times 10^{-4}\%$ of the experimental values, well within the experimental errors.

ENERGY VECTOR DEVIATION FOR VERTICALLY POLARIZED SHEAR WAVES

Having determined the texture coefficients and 'single crystal' elastic constants of 2024 aluminum for each layer of the plate, it was possible to calculate the effective orthotropic elastic moduli for each layer using Eqs. 4 and 10 of Ref. 4. A general analytic solution for the elastic wave equation has been obtained and is described elsewhere[6], permitting the phase and energy velocities and particle displacements to be calculated for arbitrary directions in the material. Using the orthotropic elastic constants and the general solution, all pertinent information can be determined for the propagation of plane elastic waves in the material.

Our main interest in this paper is the IIW type aluminum calibration block. We will restrict our consideration to vertically polarized shear waves propagating the x_1 - x_2 plane of the plate. For the rest of this discussion, we assume that the IIW block is cut from the rolled aluminum plate such that the long axis of the IIW block is parallel to the rolling direction. We also assume that the x_2 direction extends from point O, towards the edge of the quadrant, and the x_3 axis is perpendicular to the block as it is shown in Fig. 1. If the block is cut at some other angle with respect to the reference axes, the following discussion would have to be modified to reflect the different orientation.

Table I. Single crystal elastic constants and texture coefficients for layers A, B, C and D

constant layer	10^{11} dyne/cm ²			10^{-3}		
	C_{11}	C_{12}	C_{44}	W_{400}	W_{420}	W_{440}
A	10.76	6.15	2.85	9.87	-1.07	2.41
B	10.77	6.13	2.83	10.65	-1.27	3.55
C	10.75	6.13	2.84	7.75	-1.02	2.28
D	10.73	6.15	2.83	6.58	-1.13	1.52

Figures 3a and 3b show two examples of how the energy vector deviates from the phase vector in the quadrant of an IIW block when anisotropy or texture is considered. The first example (Fig. 3a) is for a single crystal aluminum block with the crystallographic axes along the x_1 and x_2 direction. The single crystal is used as both a graphic example and because it will have the 'maximum' possible texture that may be found for aluminum. The dashed lines indicate the direction of the phase vector and angles are labelled with respect to the x_1 -axis. The solid lines indicate the direction the energy travels. Single ended arrows indicate the direction and the numbers are the magnitude (degrees) the energy vector deviates from the phase vector. A chain-dash line is used at 45° to indicate that there is no deviation at that angle.

The second example (Fig. 3b) shows the same type of energy deviations, as just described, but caused by the texture of layer B. The deviation directions and magnitude are shown in the same manner as before. Since the material is orthotropic, there is a deviation at 45° , but very small. As indicated in this example, the deviations due to texture are rather small. The maximum deviation in the x_1 - x_2 plane is about 2.1. But what is the effect of this deviation on the calibration of the beam index position?

INDEX SHIFT DUE TO ENERGY VECTOR DEVIATION

To examine the index shift caused by texture, the energy direction must be considered. Since, Snell's law uses the phase direction. One must consider the tangent line to the quadrant at the point of intersection of the energy vector. By extending the phase vector to intersect the tangent line and determining the angle between the two, one can use Snell's law to determine the direction of the reflected phase vector and therefore, the direction in which the energy vector is reflected. Using this type of consideration it can be shown that in order to have the energy reflected back to the point where it entered the material (i.e., to get a maximum reflection), the phase vector must be normal to the tangent line.

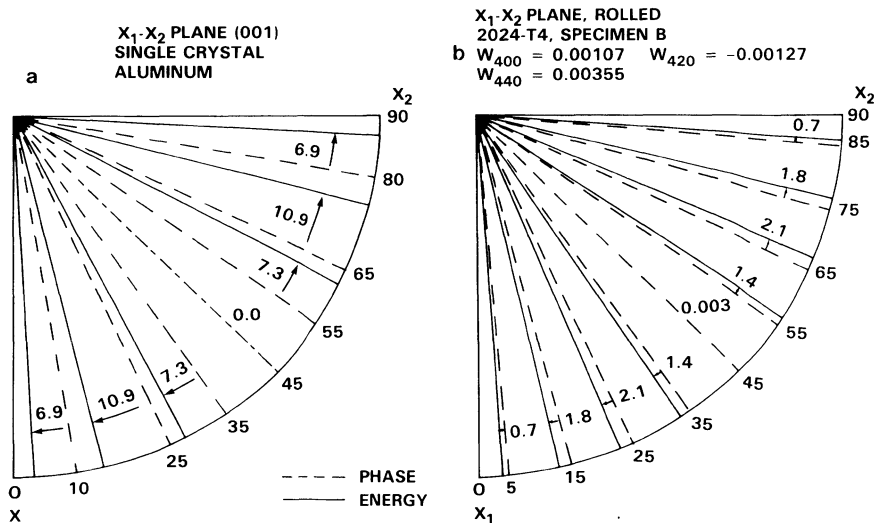


Fig. 3. Deviation of the energy from the phase vector for a number of refracted angles. a) Example for an aluminum single crystal quadrant. b) Quadrant having the same texture as layer B.

If the material is truly isotropic, the energy and phase vectors coincide. For this case (as is normally assumed for IIW calibration blocks), the acoustic waves launched at some angle from the center of the quadrant are reflected along the same path. When there is texture (and deviation of the energy from the phase vector), the point where the maximum reflection can be received will be a function of the initial direction of the waves and the point from which they were launched. In general, these two points will not coincide at the block index point (center of the quadrant) when the material has texture. The difference between the block index and position where the launch point and reflected wave coincide is the index shift.

Using the general solution for the wave equation, mentioned earlier, and the simple geometry of the quadrant, the index shift can be calculated as a function of angle. The two schematic drawings in Figs. 4a and 4b, show examples of the index shift. The first example (Fig. 4a) is for a single crystal quadrant, again for easy illustration, and shows a large index shift at 55°. The dot-dash line is the radius of the quadrant. The phase and energy vector are labelled. The index shift or Δ is -28.0 mm. The negative sign is used to indicate a shift away from the quadrant. Using the texture measured in layer B, the index shift for 75° is shown. This is the maximum index shift that was found in the x_1 - x_2 plane for any of the four layers between the angles 35° to 75°. Table II tabulates the index shift between 35° and 75° at 5° intervals for all of the layers. Although the table shows no index shift at 45°, there is a very slight shift that occurs, but it is very small and insignificant for this comparison. Also shown in Table II is that for angles less than 45° the index shift is positive or toward the curved surface of the quadrant.

DISCUSSION AND CONCLUSIONS

Experimental measurements of the index shift have yet to be made to verify the results of this analysis. However, experimental work reported by others indicates features and magnitudes of the index shift similar to those we have predicted here.[7] The aluminum alloys, texture and orientation of the blocks with respect to the rolling direction may be quite different from our material and caution must be used in the comparison. However, one notable feature is the zero index shift at 45°. This should occur for blocks oriented either parallel or perpendicular to the rolling direction.

The layer thickness for specimens A, B, C and D (type 1) was chosen for convenience. Although these are discrete layer and a texture difference can be measured, as shown in Table 1, the texture probably varies smoothly and continuously through the thickness of the plate. Two possible effects of the texture gradient are mentioned. If a narrow probe (high frequency and minimal beam spread) were to be calibrated on such a

Table II. Predicted index shifts for layers A, B, C, and D as a function of the refracted angle, at 5° intervals from 35° to 75°.

θ_r layer	35°	40°	45°	50°	55°	60°	65°	70°	75°
A	2.0	1.0	0.0	-1.5	-3.0	-5.1	-6.6	-8.6	-10.2
B	3.0	1.5	0.0	-2.0	-4.6	-6.6	-9.1	-11.7	-14.2
C	2.0	1.0	0.0	-1.5	-3.0	-4.1	-6.1	-9.7	-9.1
D	1.5	0.5	0.0	-1.0	-2.0	-3.1	-4.1	-5.1	-6.1

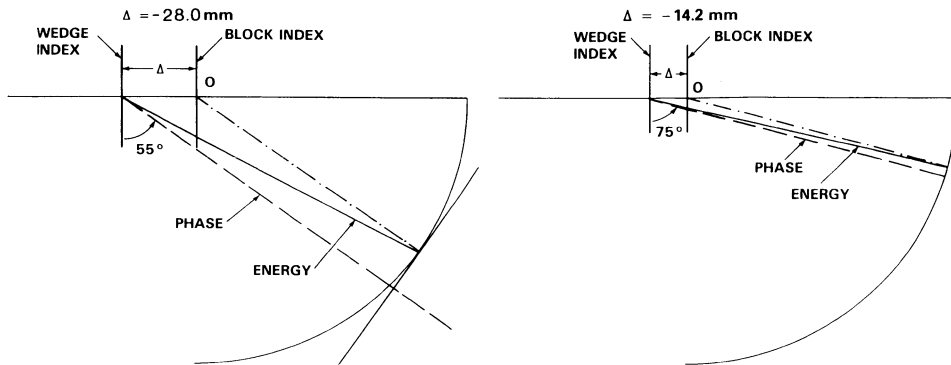


Fig. 4. Schematic drawing showing the predicted index shifts (δ) for: a) 55° probe and an aluminum single crystal quadrant, b) 75° probe and a quadrant having the texture of layer B.k

block, the index shift may vary as a function of position of the probe across the width of the calibration block. If wide probe (same high frequency and minimal beam spread) were to be used, one may see a spread or flattening of the amplitude as the probe is moved towards and away from the block index point. The index shift would be different for different areas of the transducer face. In all of the preceding work, it has been assumed that the direction of the phase vector and the point (considering rays) where the acoustic wave enters the material are known. This is the same as saying we were using calibrated transducers instead of calibrating transducers. It is the opinion of the authors that a textured IIW block must, itself, be calibrated in terms of texture before one could even consider calibrating transducers with the block.

As mentioned earlier, the maximum energy vector deviation in the x_1 - x_2 plane was 2.1° and occurred for layer B. This however was not the overall maximum deviation. The maximum deviation was approximately 4°, again for layer B. This deviation occurs for phase vectors propagating approximately at 25° and 65° with respect to the x_3 axis. These angles are accessible for angle beam inspection from the surface of the rolled plate. This implies that 'calibrating' a transducer on the same material does not guarantee the expected results. One must 'calibrate' or know the material if accuracy is desired.

REFERENCES

1. M. Brissaud and H. Kleiman, *Acustica*, **46** 168 (1980).
2. M. Brissaud and H. Kleiman, *Ultrasonics International '83* Conf. Proc., (Butterworth, Kent 1984) p. 458.
3. B. Watson, "Material for Ultrasonic Calibration Blocks," *Brit. J. of NDT*, Nov, 1985, p. 369.
4. C. M. Sayers, *J. Phys. D. : Appl. Phys.* **15**, 2157-2167 (1982).
5. M. J. P. Musgrave, *Crystal Acoustics*, (Holden-Day, SF 1970),.
6. R. B. Mignogna, *Review of Progress in Quantitative Nondestructive Evaluation Vol 8A*, Eds. D.O. Thompson and D. E. Chimenti (Plenum, NY 1989) p. 133-140.
7. H. E. Van Valkenburg and H. F. C. Hotchkings, *Abstracts 12th WCNDT, Amsterdam* p. 201 (1989) (text of poster presentation distributed by the authors as a private communication.)